agronomy

MDPI

Article

Transcriptomic Analysis of Maize Inbred Lines with Different Leaf Shapes Reveals Candidate Genes and Pathways Involved in Density Tolerance

Shulei Guo [1,2,†], Yiyang Guo [1,2,†], Jun Zhang [1], Yinghui Song [1], Jinsheng Guo [1], Liangming Wei [1], Qianjin Zhang [1], Zhenhua Wang [1], Zanping Han [2], Liru Cao [1], Xin Zhang [1] and Xiaomin Lu [1,*]

[1] Institute of Cereal Crops, Henan Academy of Agricultural Sciences, Zhengzhou 450002, China; guosl1309@163.com (S.G.); guoyiyang0830@163.com (Y.G.); zhangjun422@hotmail.com (J.Z.); yinghui820@163.com (Y.S.); guojinsheng2024@126.com (J.G.); weilm64@126.com (L.W.); zqjin@126.com (Q.Z.); wzh201@126.com (Z.W.); caoliru008@126.com (L.C.); zh5733764@126.com (X.Z.)
[2] College of Agriculture, Henan University of Science and Technology, Luoyang 471023, China; hnlyhzp@163.com
* Correspondence: luxiaomin2004@126.com
† These authors contributed equally to this work.

Abstract: Maize is an important food and feed crop. Under limited arable land area, the cultivation of high-density-tolerance crops is a key factor in promoting yield improvement. Leaf width and stalk strength are important influences on density tolerance in maize. However, no comprehensive transcriptomic analysis has focused on maize's leaf width and stalk strength formation mechanisms. In this study, comparative transcriptomic analyses demonstrated that significant transcriptome changes occurred regarding leaf width and stalk strength of narrow-leaved and wide-leaved maize inbred lines, with a total of 5001 differentially expressed genes (DEGs) identified. Enrichment analysis showed that phenylpropanoid biosynthesis, starch and sucrose metabolism, phytohormone signaling, amino acid metabolism, and brassinosteroid biosynthesis were significantly correlated with the formation of maize leaf shape and stalk strength and that the genes in these pathways were primarily involved in cell wall formation. Weighted gene co-expression network analysis identified 2 modules significantly correlated with leaf width and stalk strength, from which 11 hub genes were further identified. The 11 leaf and stem development genes in different pathways were validated using qRT-PCR. These findings can provide a theoretical basis for the mechanism of narrow-leaf and high-strength stalk formation in high-density-tolerance maize and contribute to the proposal of a breeding strategy for yield improvement.

Keywords: transcriptomic analysis; WGCNA; density tolerance; leaf width; stalk strength

check for updates

Citation: Guo, S.; Guo, Y.; Zhang, J.; Song, Y.; Guo, J.; Wei, L.; Zhang, Q.; Wang, Z.; Han, Z.; Cao, L.; et al. Transcriptomic Analysis of Maize Inbred Lines with Different Leaf Shapes Reveals Candidate Genes and Pathways Involved in Density Tolerance. *Agronomy* **2024**, *14*, 1506. https://doi.org/10.3390/agronomy14071506

Academic Editor: Enrico Porceddu

Received: 26 April 2024
Revised: 27 June 2024
Accepted: 8 July 2024
Published: 11 July 2024

Copyright: © 2024 by the authors. Licensee MDPI, Basel, Switzerland. This article is an open access article distributed under the terms and conditions of the Creative Commons Attribution (CC BY) license (https://creativecommons.org/licenses/by/4.0/).

1. Introduction

Maize (*Zea mays* L.) is an important food crop and a multipurpose crop integrating feed, oil, and processing, and its high and stable yield is crucial for food security. The increase in maize yield is largely attributed to improved tolerance to high-density planting, which produces a significant genetic gain in yield [1]. Density tolerance is a complex composite trait influenced by several factors, of which plant size and stalk quality are the main determinants of density tolerance in maize [2]. Leaf size and morphology not only determine population canopy structure but are also key components of desirable density-tolerance plants. When planted densely, wider leaves often lead to shade avoidance syndrome. The risk of lodging is increased by the thinness and poor quality of the plant's stalks and increasing the mechanical strength of the basal 3rd–4th nodes of the stalks enhances the plant's lodging resistance [3,4]. Leaf width, as a key component of leaf size and morphology, is closely related to leaf structural properties. Leaf width was significantly

negatively correlated with mesophyll conductance and stomatal density, as well as with water use efficiency while being positively associated with stomatal conductance; the wider the leaf, the lower the stomatal density and mesophyll conductance [5,6]. To maintain high photosynthetic rates, stomata need to be enlarged for increased stomatal conductance to CO_2, but this also leads to increased transpiration, which reduces water use efficiency [7]. The appropriate reduction in leaf width was able to reduce population transpiration and the shading effect of the lower and middle leaves without affecting photosynthetic products and seed yield [4,8]. Increasing population water use efficiency by reducing leaf transpiration is an important option for crop improvement, as is the ability of narrow leaves to reduce leaf transpiration by decreasing leaf area, and thus narrow leaves may be an important breeding target.

It is important to explore the related genes and regulatory networks for the formation of leaf width and stalk strength to increase planting density. Qi et al. revealed that the rice genes *NAL2* and *NAL3* are homologs of the maize leaf shape-related genes *NS1* and *NS2*, respectively, and that *NAL1*, *NAL2*, and *NAL3* regulate leaf width and plant height by affecting the formation of leaf veins and cell division of meristematic tissues at the base of the stalk [9]. The cellulose synthase *OsCSLD4* encodes the type II enzyme GT2 belonging to the glycosyltransferase family 2, which regulates leaf width and plant height by affecting cell division [10], and *ZmCLSD1* has the same function [11]. The AP2-type transcription factor DIL1 regulates maize internode length and leaf shape [12]. Mutations in the *VT2* gene, which encodes a tryptophan aminotransferase, affect IAA synthesis and lead to shortened internodes in maize [13]. The maize *brachytic2* (*br2*) and *ZmPIN1a* regulate stalk thickness increase and internode shortening by mediating polar auxin transport [14,15], and *ZmPIN1a* also affects plant height reduction and root enlargement and improves resistance to collapse [16]. The *OsFLN1* and *OsFLN2* genes encode pfkb-type carbohydrate kinases that regulate leaf and plant height formation by affecting chloroplast development [17,18]. In dwarf and narrow-leaf (*dnl4*) mutants, the expression of leaf growth-related genes such as *NAL1* and *NAL7* was down-regulated [19]. Mutations in the *dnl2* gene cause a significant reduction in auxin and gibberellin content, which inhibits cell growth and affects structural alterations in the vascular bundles and secondary cell walls, leading to dwarf and narrow-leaf phenotypes in maize [20].

Currently, the lack of genetic resources related to maize densification is significantly limiting maize yield improvement. In this study, a comparative transcriptome sequencing and analysis was performed using leaves and stalks of narrow-leaved and wide-leaved maize inbred lines, which were combined with data on density tolerance to identify hub genes related to leaf width and stalk strength, providing genetic resources and theoretical bases for improving maize's ability to adapt to high-density planting.

2. Materials and Methods

2.1. Plant Materials and Trait Survey

Narrow-leaved maize inbred line NL409 is a European hybrid bred resulting from continuous self-crossing, and wide-leaved maize inbred line WB665 is derived from a cross between Chang 7-2 and Zhengdan 958, selected by continuous self-crossing. Both were planted in the experimental fields of the Henan Academy of Agricultural Sciences, three planting densities (82,500 plants/hm^2, 112,500 plants/hm^2, and 150,000 plants/hm^2) were set, and each density containing three plot replicates. Each plot consists of five rows, each five meters long.

At the 9-leaf stage of maize, traits of NL409 and WB665 at three planting densities were measured, including leaf length, leaf width, leaf length-to-width ratio, leaf puncture strength, and content of indole-3-acetic acid (IAA), gibberellin (GA), brassinolide (BL), and 6-deoxocastasterone (6DCS). Leaf length was determined from the beginning of the ligula to the tip of the leaf. Leaf width was measured across the widest portion of the leaves. Leaf puncture strength was determined with a YYD-1 instrument (Zhejiang Top Instrument Co. Ltd., Zhejiang, China) [21]. These leaf traits were measured for 10 plants per replicate.

Three replicates of IAA, GA, BL, and 6DCS samples were collected from each line at the density of 82,500 plants/hm^2, and three plants were mixed into one replicate. The samples were quick-frozen with liquid nitrogen and stored at −80 °C. An Agilent1290 (Agilent, Santa Clara, CA, USA) high-performance liquid chromatography (HPLC) coupled with the AB Qtrap6500 mass spectrometer (Framingham, MA, USA) was used to detect IAA, GA, BL, and 6DCS [22].

Traits of the 3rd to 4th internode on the ground of NL409 and WB665 at three planting densities were also measured, including stalk internode length, stalk internode thickness, stalk puncture strength, stalk breaking strength, and content of lignin, cellulose, and hemicellulose. The 3rd to 4th internode length and internode thickness were measured with straightedge and vernier calipers, respectively. Stalk puncture strength and stalk breaking strength were also determined at the 3rd to 4th internode using a YYD-1 instrument. The measured stalk traits were the average values of the 3rd to 4th internode of 10 plants per replicate. Three biological replicates of lignin, cellulose, and hemicellulose samples were collected from each line at a density of 82,500 plants/hm^2, and three plants were mixed for one replicate. These samples were immediately enzyme deactivated at 105 °C for 30 min in an air-drying oven and then air-dried naturally. Dried stalk samples were ground and filtered through an 80-mesh screen (0.180 mm fineness). The determination of cellulose, hemicellulose, and lignin in air-dried filtered samples was performed using an Agilent1290 high-performance liquid chromatography (HPLC) system [23]. Traits were measured at the time of maize harvest including plant height, ear height, and yield. The usual planting density of 82,500 plants/hm^2 was used as the yield CK group. Student's *t*-test was performed to show the significance between two inbred lines using Microsoft Excel 2010 software.

At the 9-leaf stage of maize, the 9th leaf and the 3rd to 4th nodes of stalks on the ground of maize planted under the density conditions of 82,500 plants/hm^2 were selected as samples, which were frozen and stored in liquid nitrogen for transcriptome sequencing. Three biological replicates, each of which were pooled from three plants, were collected per material per organ.

2.2. RNA Library Construction and Sequencing

The RNA Prepure Plant Kit (TIANGEN, Beijing, China) was used to isolate RNA from the leaves and stalks of 12 samples (NL409 and WB665). RNA quality was assessed using the Agilent 2100 Bioanalyzer (Agilent Technologies, Palo Alto, CA, USA) and NanoDrop 2000 (IMPLEN, Westlake Village, CA, USA). The total RNA of each sample was then used to construct RNA-seq libraries using the NEBNext Ultra RNA Library Prep Kit for Illumina (NEB, Ipswich, MA, USA) following the manufacturer's protocols. RNA-seq was conducted on the Illumina HiSeq X Ten platform to obtain raw reads.

2.3. Identification and Functional Annotation of DEGs

Using FastQC software (version 0.11.5) [24], the obtained raw reads were filtered to remove the sequences containing splices, low quality ($Q_{phred} < 30$), and those containing N percentages greater than 5% to obtain high-quality clean reads. Clean reads were then mapped to the maize B73 reference genome V4 (AGPv4) [25] using Hisat2 (v2.0.5) [26]. The level of gene expression was measured by FPKM (Fragments Per Kilobase of exon model per Million mapped fragments) [27]. The DESeq2 (v1.16.1) [28] was used to identify differentially expressed genes (DEGs) with the criteria of *q*-values (the *p*-values were adjusted using a false discovery rate) < 0.05 and |log2 FC (fold change)| > 1. Gene Ontology (GO) functional enrichment analysis and Kyoto Encyclopedia of Genes and Genomes (KEGG) pathway enrichment analysis of DEGs were performed using clusterProfiler (v3.4.4) package [29].

2.4. Gene Network Construction and Screening of Hub Genes

Co-expression networks were built using the WGCNA (v1.6.6) package [30] based on the FPKM values of the DEGs. The modules were produced according to the default settings, except for the following parameter: power (9). Power is the soft threshold, which is calculated according to the pickSoftThreshold function and can reflect whether the correlation value is close to the scale-free network feature. The best power value in this WGCNA analysis is 9. The hub genes were selected based on the module KME values (KME > 0.8) and high-weight values (GS > 0.3). Cytoscape (v3.4.0) was used to draw networks.

2.5. Quantitative RT-PCR Analysis

To validate the DEGs detected by RNA-seq sequencing, 11 genes related to leaf and stalk formation were selected for qRT-PCR analysis. qRT-PCR was carried out using the GoTaq qPCR Master Mix Kit M7123 (Promega (Beijing) Biotech Co., Ltd, Beijing, China) on Bio-Rad CFX96 real-time fluorescence quantifier, with the following program: 95 °C for 3 min, 95 °C for 10 s, 60 °C for 15 s, and fluorescence collection: 42 cycles. All primers used for the validation experiments were designed with Primer Premier 5 software and are shown in Supplementary Table S1. The 18SrRNA (LOC111590468) in maize was used as an internal control to normalize the measured gene expression levels [31]. The relative expression levels of genes were calculated using the $2^{-\Delta\Delta}$CT method with three biological replicates and three technical replicates [32], and three individual plants mixed for each biological replicate. Pearson correlation analysis was performed between qRT-PCR value and RNAseq value using Microsoft Excel 2010 software.

3. Results

3.1. Results of Leaf and Stalk Trait Analysis

An analysis of leaf and stalk trait data from the narrow-leaved maize inbred line NL409 and the wide-leaved maize inbred line WB665 revealed that the levels of all four hormones (IAA, GA, BL, and 6DCS) were significantly lower in NL409 than that in WB665 at the 9-leaf stage of maize (Table 1). Four phenotypic parameters of leaves and seven phenotypic parameters of stalks were determined, and it was found that the average leaf width, leaf puncture strength, ear height, and ear-position-to-plant-height ratio of NL409 were significantly lower than those of WB665, whereas the leaf length, leaf length-to-width ratio, and plant height were significantly higher than those of WB665; the stalk internode length, the stalk internode thickness, the stalk puncture strength, and the stalk breaking strength of the third to fourth nodes above ground of NL409 were significantly higher than those of WB665 (Figure 1, Table 1). In addition, the lignin, cellulose, and hemicellulose contents of the third to fourth nodes on the ground of NL409 and WB665 were determined, and it was found that the cellulose and hemicellulose contents of NL409 were significantly higher than that of WB665, whereas there was no significant difference in lignin content (Table 1).

Table 1. Leaf and stalk phenotypic traits of inbred liness NL409 and WB665.

Trait	NL409	WB665
leaf width (cm)	4.08 ± 0.16 A	7.97 ± 0.36 B
leaf length (cm)	62.07 ± 2.69 A	51.06 ± 2.73 B
Leaf length-to-width ratio	15.23 ± 0.58 A	6.41 ± 0.27 B
Leaf puncture strength (N/mm^2)	6.33 ± 1.06 A	7.50 ± 1.54 B
IAA (ng/g)	25.60 ± 0.62 A	49.61 ± 0.38 B
GA (μg/g)	0.785 ± 0.01 A	0.814 ± 0.01 B
BL (ng/g)	0.009 ± 0.00 A	0.022 ± 0.00 B
6DCS (ng/g)	0.046 ± 0.00 A	1.379 ± 0.01 B
Stalk internode long (cm)	14.49 ± 2.42 Aa	12.91 ± 1.90 Ab

Table 1. *Cont.*

Trait	NL409	WB665
Stalk internode thickness (cm)	6.61 ± 0.48 A	5.83 ± 0.20 B
Internode length-to-thickness ratio	2.21 ± 0.44 a	2.22 ± 0.35 a
Plant height (cm)	163.85 ± 10.43 A	126.75 ± 6.91 B
Ear height (cm)	49.50 ± 5.93 A	55.03 ± 5.83 B
Plant height-to-ear position ratio	0.30 ± 0.04 A	0.43 ± 0.04 B
Stalk puncture strength (N/mm^2)	32.41 ± 4.00 A	29.63 ± 3.53 B
Stalk breaking strength (N/mm^2)	296.35 ± 51.92 A	218.77 ± 41.92 B
Lignin (mg/g)	123.47 ± 17.54 a	129.45 ± 17.13 a
Cellulose (mg/g)	564.34 ± 37.32 A	462.71 ± 40.37 B
Hemicellulose (mg/g)	255.31 ± 21.99 A	194.7 ± 34.14 B

IAA, GA, BL, 6DCS, Lignin, Cellulose, and Hemicellulose values are the means ± SD of three biological replicates for each of the narrow-leaved maize inbred line NL409 and the wide-leaved maize inbred line WB665 at a density of 82,500 plants hm^{-2}, and three individual plants were mixed into one replicate. Agronomic trait values are the means ± SD of three biological replicates for each inbred line NL409 and WB665 at a density of 82,500 plants hm^{-2}, with each replicate containing ten individual plants. Different upper and lower letters indicate significant differences at 0.01 and 0.05 levels, respectively.

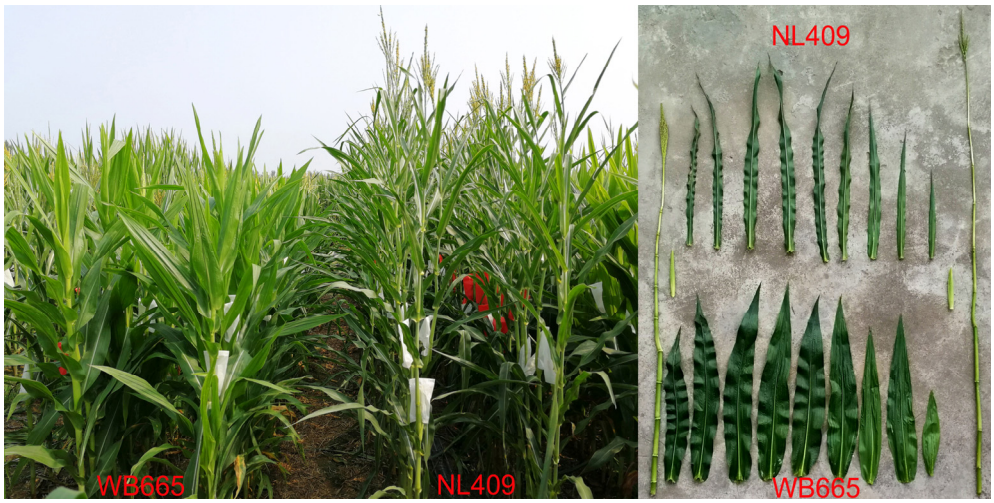


Figure 1. Phenotypes of wide-leaved maize inbred line WB665 and narrow-leaved maize inbred line NL409 in the field and of single plants.

Under the same density planting condition, the yield of narrow-leaved maize inbred line NL409 was always significantly higher than that of wide-leaved maize inbred line WB665, and the yield increase ratio of NL409 was also always significantly higher than that of WB665 when the planting density increased (Table 2), which revealed that the density tolerance of NL409 was superior under high-density conditions.

Table 2. Yield of inbred lines NL409 and WB665 at different densities.

Density	Yield (kg)		Yield Increase Ratio (%)	
	NL409	WB665	NL409	WB665
82,500 plants hm^{-2}	2210.78 ± 5.77 A	886.28 ± 2.96 B	0	0
112,500 plants hm^{-2}	2595.03 ± 4.68 A	1022.46 ± 3.01 B	17.38	15.36
150,000 plants hm^{-2}	2804.92 ± 4.81 A	1003.91 ± 1.85 B	26.87	13.27

Values are the means ± SD of three biological repeats for each of the narrow-leaved maize inbred line NL409 and the wide-leaved maize inbred line WB665. Different upper letters indicate significant differences in yield at the 0.01 level of the same density.

3.2. Identification of DEGs in Leaves and Stalks between NL409 and WB665

The number of clean reads of each sample after filtering was between 40,071,256 and 58,766,686 (Supplementary Table S2). The GC percentage of each sample was between

53.54% and 55.29% and the Q30 was between 92.61% and 95.18% (Supplementary Table S2), and principal component analysis (PCA) was performed to reveal variation and relationships among samples. (Figure 2A), indicating that the sequencing quality was high and suitable for subsequent analysis. Pairwise comparisons between the leaf (NLL: Narrow-leaved NL409 leaf; WLL: Wide-leaved WB665 leaf) and the stalk (NLS: Narrow-leaved NL409 stalk; WLS: Wide-leaved WB665 stalk) individuals of narrow-leaved NL409 and wide-leaved WB665 were performed to examine their transcriptomic changes. In total, 9060 leaf-DEGs (LDEGs) (Supplementary Table S3) and 9539 stalk-DEGs (SDEGs) (Supplementary Table S4) were identified in leaves and stalks, respectively, in a comparison of NL409 and WB665 (Figure 2B). The set of differential genes for leaves and stalks was taken as the intersection and 5001 DEGs were obtained (Figure 2B). Volcano plots displaying the up-regulated, down-regulated, and non-regulated genes in leaves and stalks between NL409 and WB665 (Figure 2C,D).

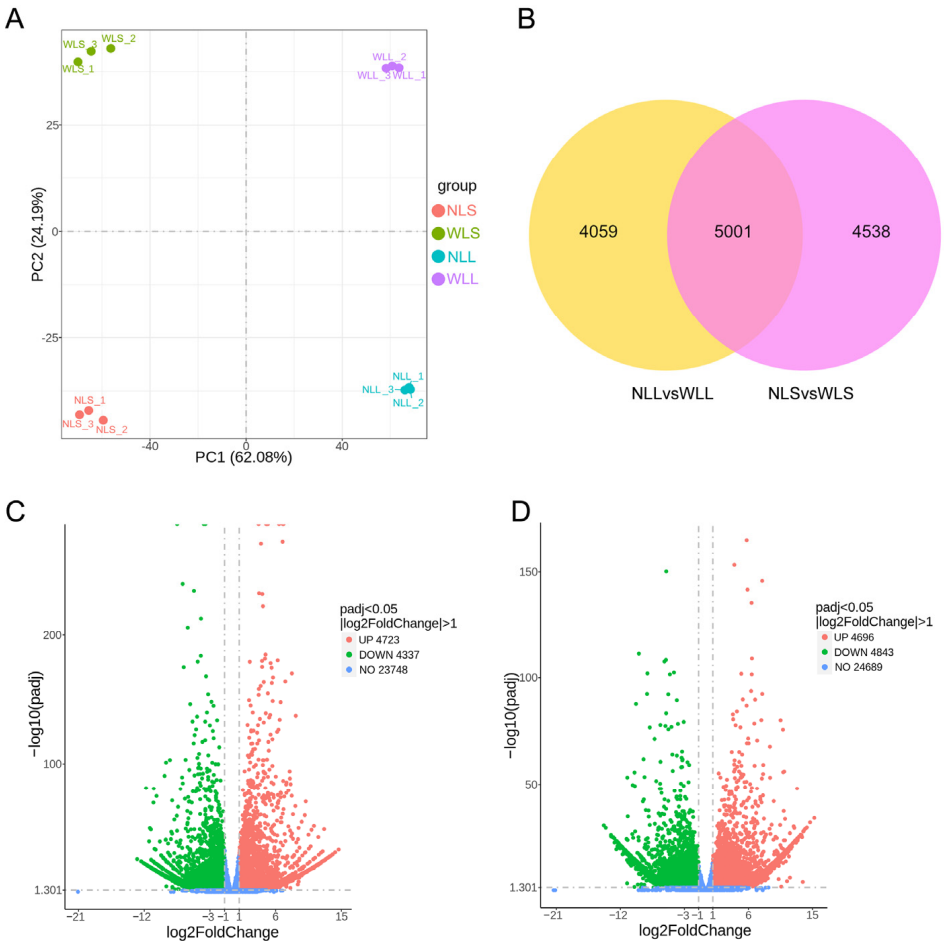


Figure 2. PCA Analysis of transcriptome data and DEGs in leaves and stalks between the narrow-leaved maize inbred line NL409 and the wide-leaved maize inbred line WB665. (**A**) Samples from the same group have the same color in the PCA analysis. (**B**) Venn diagram shows the number of DEGs in leaves and stalks between NL409 and WB665. (**C**) Volcano plots display the up-regulated, down-regulated, and non-regulated genes in leaves between NL409 and WB665. (**D**) Volcano plots displaying the up-regulated, down-regulated, and non-regulated genes in stem between NL409 and WB665.

3.3. GO Functional Enrichment Analysis and KEGG Pathway Enrichment Analysis of DEGs

GO enrichment analysis of DEGs was performed to determine the functions of the distinct transcripts differentially expressed in the leaf and stalk. In the leaf, 9060 LDEGs were found to be significantly enriched for 20 GO terms containing 7 biological processes,

1 cellular component, and 13 molecular functions (q-value < 0.05). In the stalk, 9539 SDEGs were found to be significantly enriched for 20 GO terms containing 9 biological processes, 1 cellular component, and 10 molecular functions (q-value < 0.05). The biological processes (BPs) that were significantly enriched in both leaves and stalks were protein phosphorylation (GO:0006468) and response to other organisms (GO:0051707) (Figure 3). The cellular component (CC) that was significantly enriched in both leaves and stalks was the plasma membrane (GO:0005886) (Figure 3). The molecular functions (MFs) that were significantly enriched in both leaves and stalks were categorized into six GO entries such as protein serine kinase activity (GO:0106310), iron ion binding (GO:0005506), protein serine/threonine kinase activity (GO:0004674), polysaccharide binding (GO:0030247), heme binding (GO:0020037), and transmembrane transporter activity (GO:0022857) (Figure 3). The unique significantly enriched GO terms in leaves showed a high number of down-regulated genes, such as the lignin biosynthetic process (GO:0009809) and cell surface receptor signaling pathway (GO:0007166), while there were more up-regulated genes with transmembrane receptor protein serine/threonine kinase activity (GO:0004675), monooxygenase activity (GO:0004497), and ADP binding (GO:0043531). GO items were only significantly enriched in stems, such as the lipid catabolic process (GO:0016042), the response to sucrose (GO:0009744), and the regulation of jasmonic acid-mediated signaling pathway (GO:2000022) with more up-regulated genes, whereas the more down-regulated gene was transcription cis-regulatory region binding (GO:0009809). The genes contained in these entries may play an important role in the formation of leaves and stalks.

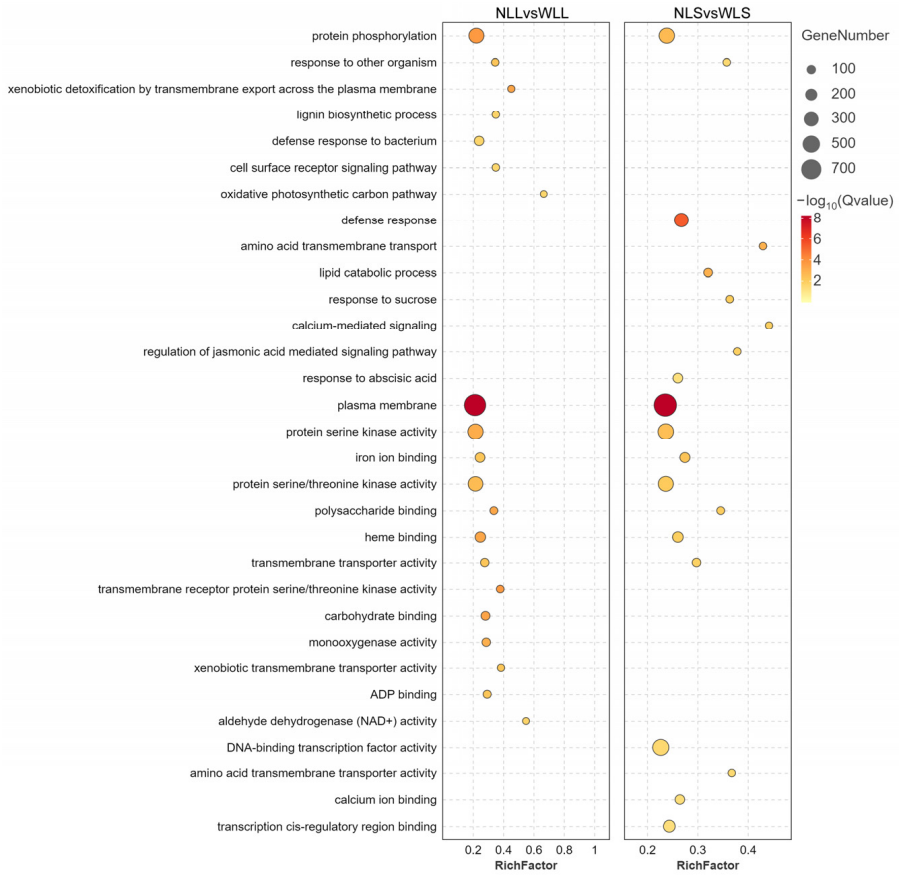


Figure 3. Gene ontology enrichment analysis of DEGs identified in leaves and stalks between the narrow-leaved maize inbred line NL409 and the wide-leaved maize inbred line WB665. NLL: Narrow-leaved NL409 leaf; WLL: Wide-leaved WB665 leaf; NLS: Narrow-leaved NL409 stalk; WLS: Wide-leaved WB665 stalk. The number of DEGs in each GO term is positively related to the size of plot, and the corresponding $-\log_{10}$(Qvalue) of each entry shown in red is more significant.

KEGG enrichment analysis was performed to identify pathways enriched for DEGs in the leaf and stalk. In the leaf, 9060 LDEGs were significantly enriched in 16 pathways including starch and sucrose metabolism, phenylpropanoid biosynthesis, diterpenoid biosynthesis, and brassinosteroid biosynthesis (p-value < 0.05) (Figure 4). In stalk, 9539 SDEGs were significantly enriched in 15 pathways including α-linolenic acid metabolism, Alanine, aspartate and glutamate metabolism, plant–pathogen interaction, and plant hormone signal transduction (p-value < 0.05) (Figure 4). A total of seven pathways were co-enriched in leaves and stalks, including the α-linolenic acid metabolism pathway, the cysteine and methionine metabolism pathway, the biosynthesis of various plant secondary metabolites pathway, the starch and sucrose metabolism pathway, the phenylpropanoid biosynthesis pathway, and alanine, aspartate, and glutamate metabolism pathways, in which the number of up-regulated and down-regulated genes were significantly different between leaves and stalks (Supplementary Table S6). The genes in the above pathways may be closely related to leaf morphology and stalk strength.

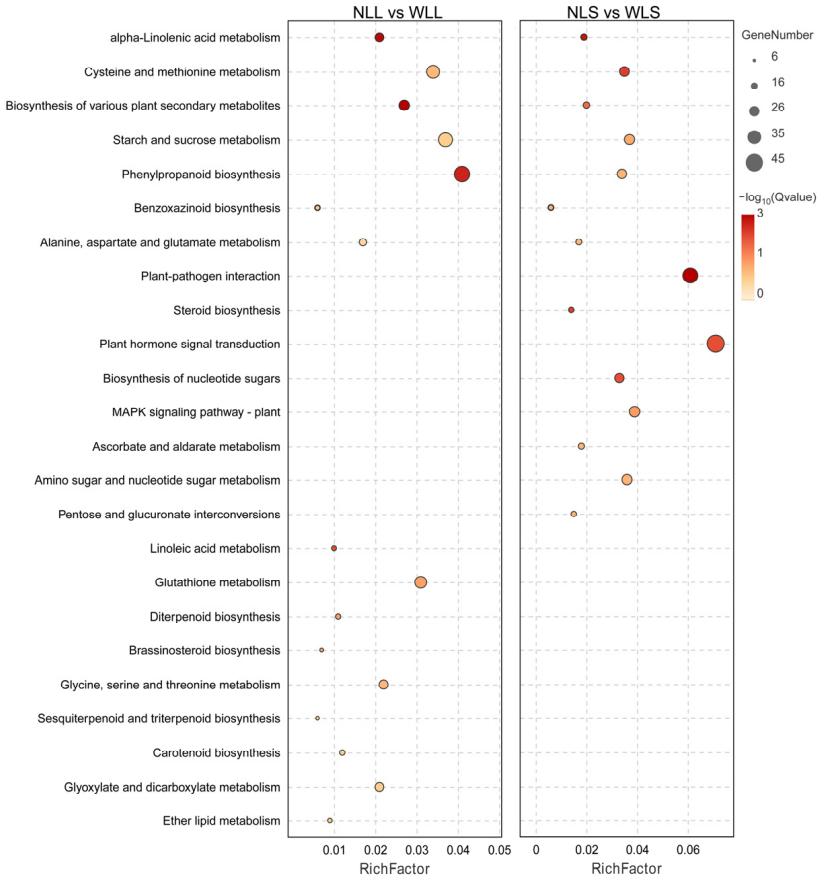


Figure 4. KEGG analysis of DEGs identified in leaves and stalks between the narrow-leaved maize inbred line NL409 and the wide-leaved maize inbred line WB665. NLL: Narrow-leaved NL409 leaf; WLL: Wide-leaved WB665 leaf; NLS: Narrow-leaved NL409 stalk; WLS: Wide-leaved WB665 stalk. The number of DEGs in each pathway is positively related to the size of plot, and the corresponding $-\log_{10}$(Qvalue) of each entry shown in red is more significant.

The intersection of the DEGs obtained from the GO and KEGG enrichment analyses described above was taken, and a total of 61 unique LDEGs containing 16 DEGs were found to be shared between the leaves of NL409 and WB665, which were mainly involved in functions such as brassinosteroid biosynthesis, carotenoid biosynthesis, diterpenoid biosynthesis, glycine, serine and threonine metabolism, glutathione metabolism, and phenylpropanoid biosynthesis (Supplementary Table S7). Similarly, there were only 102 unique SDEGs containing 23 DEGs found to be shared between the stalks of NL409 and

WB665, which were mainly involved in the functions of plant hormone signal transduction, plant–pathogen interaction, phenylpropanoid biosynthesis, and steroid biosynthesis (Supplementary Table S7). In addition, 22 DEGs were identified in both leaves and stalks. These genes mentioned above may play an important role in the formation of leaf morphology and stalk strength.

3.4. Weighted Gene Co-Expression Network Analysis

Weighted gene co-expression network analysis (WGCNA) was carried out using 20,876 genes identified in leaves and stalks between the narrow-leaved maize inbred line NL409 and the wide-leaved maize inbred line WB665 (Figure 5A). These DEGs were divided into nine different modules, and the number of genes contained in each module varied considerably, with the Turquoise module having the highest number of genes at 4975 and the Grey module having the lowest number of genes at 9 (Figure 5B). The correlations between the modules and the samples were analyzed, and it was found that the Red module was negatively correlated with both leaves and stalks in NL409 and positively correlated with both leaves and stalks in WB665, while the Turquoise module was positively correlated with both leaves in NL409 and WB665 and negatively correlated with stalks in both NL409 and WB665 (Figure 5C). We hypothesize that the genes contained in the Red and Turquoise modules may be closely related to the formation of leaf morphology and stalk strength.

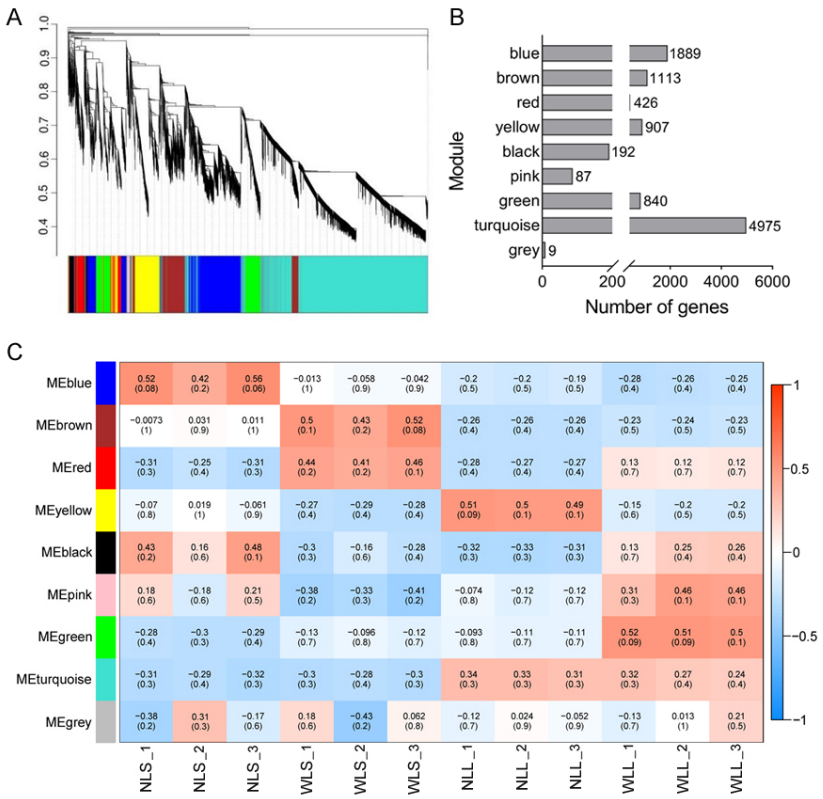


Figure 5. WGCNA analysis of DEGs identified in leaves and stalks between the narrow-leaved maize inbred line NL409 and the wide-leaved maize inbred line WB665. (**A**) The hierarchical clustering tree of co-expression modules was generated by WGCNA. (**B**) The number of genes in each module. The upper and lower breakpoints in the *x*-axis are 400 and 200, respectively. (**C**) The correlation between module and trait. Each row represents a module and each column corresponds to a sample. The numbers in each rectangular box represent the correlation coefficient (**top**) and the corresponding *p*-value (**bottom**). Red represents a positive correlation and blue represents a negative correlation between the module and the trait.

To resolve the biological functions of the genes in the modules, KEGG enrichment analysis was performed on genes in the Red and Turquoise modules. The results showed that genes in the Turquoise module were significantly enriched to pathways including aminoacyl-tRNA biosynthesis, carbon metabolism, carbon fixation in photosynthetic organisms, amino acid biosynthesis, secondary metabolite biosynthesis, and the pentose phosphate pathway (Figure 6A). The genes in the Red module were significantly enriched to pathways including ribosome (Figure 6B). The hub genes were identified by constructing gene co-expression networks, and finally, 206 DEGs were identified in the Turquoise and Red modules, from which the genes with connectivity weight $\geq$0.55 were further screened, and the interaction networks were visualized using Cytoscape software (v.3.0.2) to uncover a total of 11 hub genes (Figure 7).

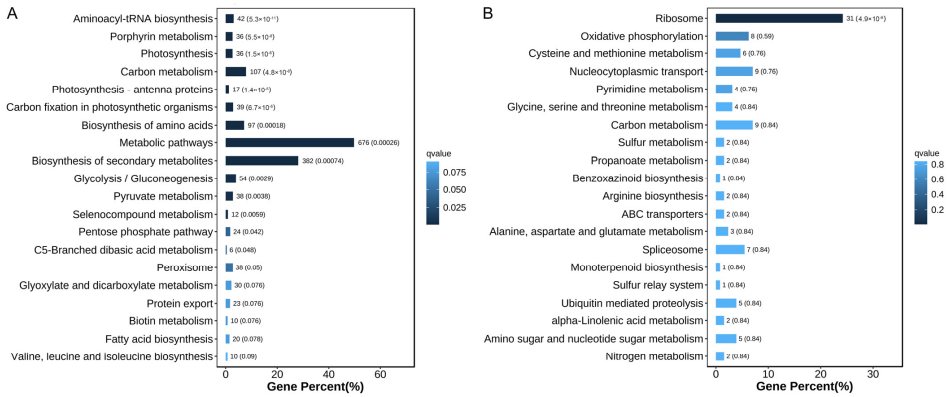


Figure 6. KEGG analysis was performed on genes related to leaves and stalks in the Red and Turquoise modules obtained from WGCNA analysis. (**A**) KEGG analysis of genes related to leaves and stalks in the Red module. (**B**) KEGG analysis of genes related to leaves and stalks in the Turquoise module.

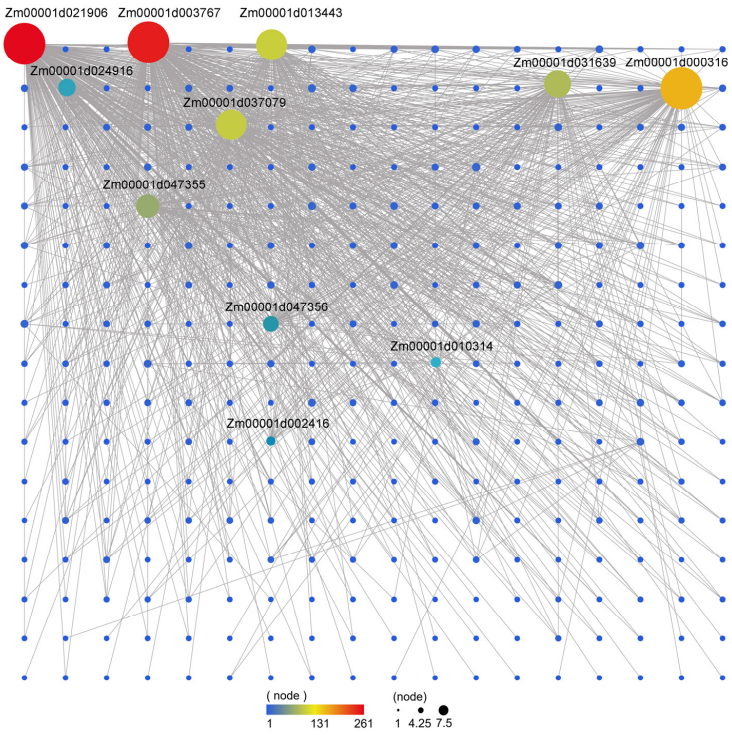


Figure 7. Co-expression network analysis results of the 11 hub genes in the Red and Turquoise modules. Each circle represents a hub gene. Circle size and color represent the degree. Line size represents the weight.

3.5. Validation of Differentially Expressed Genes by qRT-PCR

The expression patterns of 11 genes related to leaf and stem development were validated using qRT-PCR, including 3 genes (Zm00001d036959, Zm00001d005421, and Zm00001d009795) related to stalk strength, 2 TCP (Teosinte Branched1/CYCLOIDEA/Proliferating cell factor) genes (Zm00001d039371 and Zm00001d007868), 2 IAA genes (Zm00001d023704 and Zm00001d027759), 1 GA gene (Zm00001d016973), 1 lignin biosynthesis gene (Zm00001d037547), and 2 hub genes (Zm00001d000316 and Zm00001d013443). All these genes revealed the same expression trend between the qRT-PCR result and the RNA-Seq result (Figure 8), which confirmed the reliability of the RNA-seq result.

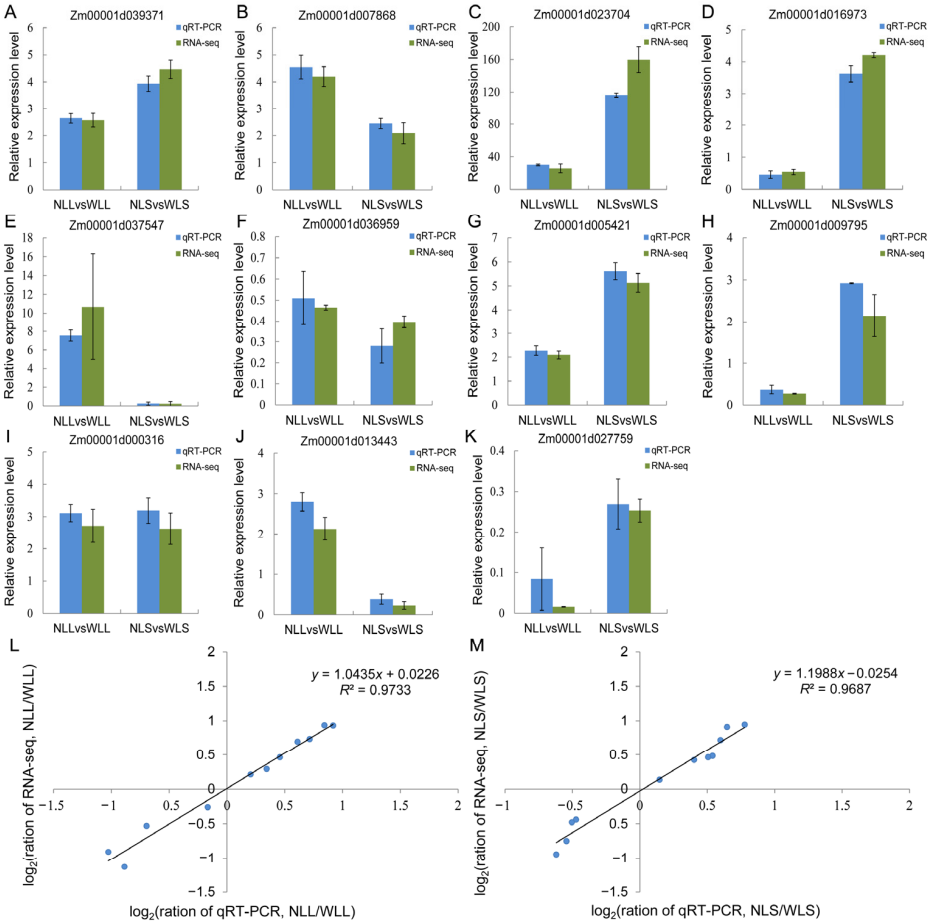


Figure 8. qRT-PCR validation of transcriptome sequencing. (**A**–**K**) The expression profiles of 11 validated genes, respectively; (**L**–**M**) the correlation diagram of validated genes detected by RNAseq and quantitative real-time PCR in leaves and stems, respectively. The *X*-axis value and *Y*-axis value corresponding to the blue dots represent the qRT-PCR value and RNAseq value of each validated gene, respectively. Error bars represent the standard error of the means of three biological and three technical replicates. NLL: Narrow-leaved NL409 leaf; WLL: Wide-leaved WB665 leaf; NLS: Narrow-leaved NL409 stalk; WLS: Wide-leaved WB665 stalk.

4. Discussion

4.1. Excellent Density Tolerance Contributes to High Maize Yields

Cellulose is the main structural component of plant cell walls, usually combined with hemicellulose and lignin, and directly affects the mechanical strength of maize stalks. Previous researchers have noted a strong stalk and lower ear–plant height ratio increase in resistance to stalk lodging, which not only prevents production losses from stalk lodging but also greatly enhances the high-density tolerance under stress conditions [33,34]. Similar results were observed in this study. We found that the stalk strength of NL409

was significantly higher than that of WB665, which may be due to the significantly higher internode thickness and cellulose and hemicellulose content of NL409 than that of WB665 (Table 1). According to these results, the stalk thickness, cellulose, and hemicellulose content of cell walls were related to the mechanical strength of the stalk, similar to the findings of previous researchers [33–35]. In addition, NL409 has a lower center of gravity (ear-position-to-plant-height ratio) and narrower leaf width compared to WB665. Therefore, this superior tolerance to density contributed to higher yields of NL409 under high-density planting conditions.

4.2. Regulatory Pathways Affecting Leaf and Stalk Development and Formation

The growth and development of leaves and stalks in plants are related to many factors, and it has been reported that plant hormone signal transduction and metabolism play a crucial role in determining maize leaf and stem formation by regulating cell division and cell elongation [9,36]. In the present study, multiple phytohormone signaling pathways associated with leaf and stalk development were significantly enriched for many hormone genes (Figure 9; Supplementary Table S8), such as GA, BR, and IAA, which is consistent with previous research [20]. When the DELLA gene is highly expressed, it inhibits internal GA signaling and stalk elongation [37,38]. Consistent with these prior findings, the DELLA family genes Zm00001d042472 and Zm00001d042127 were up-regulated (Supplementary Table S8), resulting in the down-regulated expression of downstream genes and suppression of GA content (Figure 9C; Table 1). However, the inhibition of stalk elongation was not observed. Knockdown of the GA-insensitive dwarfing gene, Zm00001d016973, resulted in a reduction in leaf vascular bundles, affecting leaf droop [39]. In this paper, Zm00001d016973 was specifically up-regulated in stalks (Figure 9C), which may cause an increase in vascular bundles, resulting in enhanced stalk strength of NL409.

TCP (Teosinte Branched1/CYCLOIDEA/Proliferating cell factor) genes in the BR signaling pathway are essential to regulating plant growth and development by promoting cell division [40–43]. In our study, the *TCP2* (Zm00001d007868), *TCP3* (Zm00001d038683), and *TCP4* (Zm00001d039371) genes were up-regulated (Supplementary Table S8), resulting in the down-regulated expression of genes in the auxin pathway (Figure 9A; Supplementary Table S9), similar to the findings of previous studies [41,43]. The down-regulated expression of *CYC10* (CYCLOIDEA, Zm00001d019696) (Figure 9B) was consistent with the lower BR content in NL409 (Table 1) and the inhibition of leaf development [40,42]. *ARF2* is a repressor of cell division and organ size [44], and *ARF2* (Zm00001d023704) was up-regulated in leaves (Figure 9A), which may be associated with the suppression of leaf width. ARF can bind specifically to the auxin response element (AuxRE) [45], and a large number of these elements were present in BR genes (Supplementary Table S9; Supplementary Figure S1). The number of genes up-regulated and down-regulated in the auxin and brassinosteroid pathways differed markedly in leaves and stalks (Figure 9; Supplementary Table S9). Thus, we speculate that the molecular transduction pathways for developmental signals are not linear but are rather linked through a complex network, and the genes involved in the same pathway in different organs are variable.

Studies have shown that the expression of genes involved in cellulose, hemicellulose, and lignin biosynthesis pathways plays an important role in cell wall structure and stalk strength, and up-regulated expression of these genes tends to improve maize stalks to resist collapse [46,47]. Our study also found that seventeen cellulose, hemicellulose, and lignin candidate genes were identified in stalks, 13 of which were up-regulated in NL409 (Supplementary Table S10). This result is consistent with previous studies. Additionally, most of the identified genes mediating cell wall loosening and hydrolysis were down-regulated expression (Supplementary Table S11), which reduces hemicellulose deposition in the secondary cell wall [47]. In summary, the differences in the expression of these genes may be responsible for the higher stalk strength of narrow-leaved maize inbred line NL409 compared to wide-leaved maize inbred line WB665.

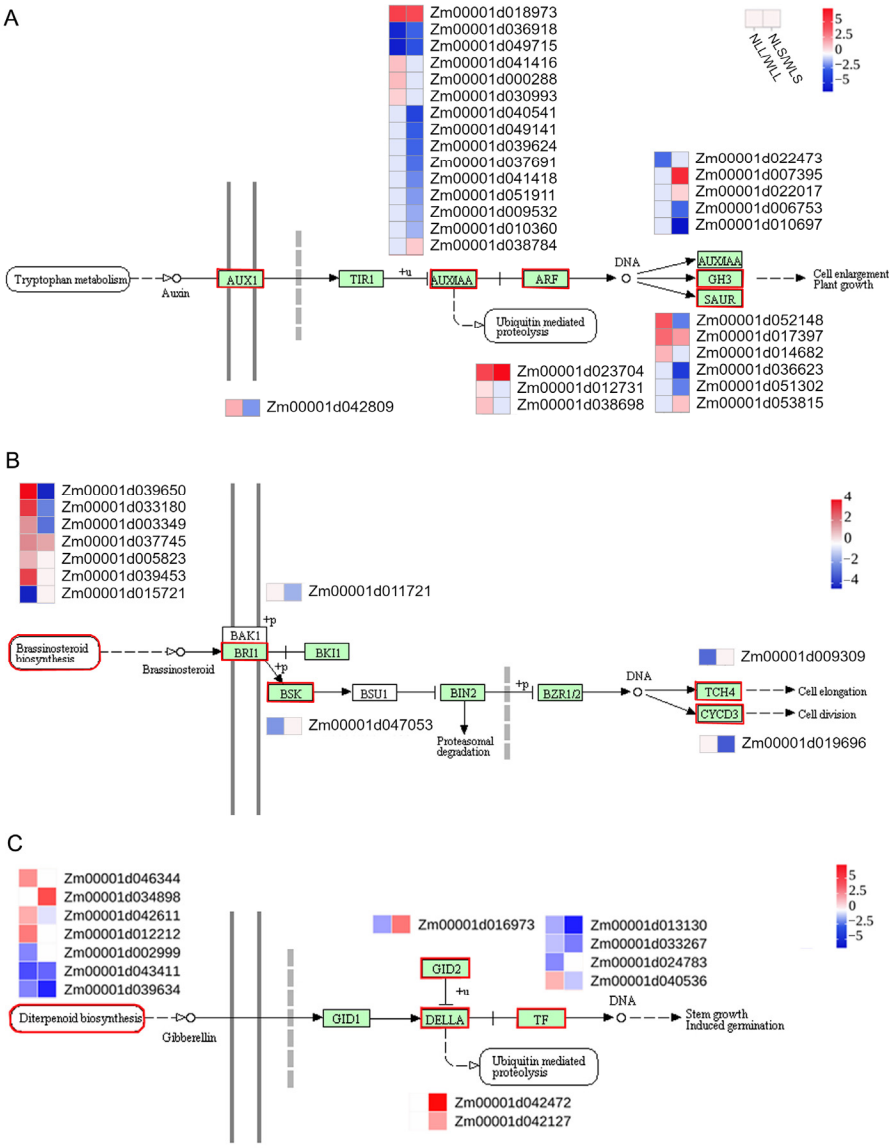


Figure 9. Auxin and brassinolide pathway enrichment genes. (**A**) The expression of auxin pathway enrichment genes in leaves and stalks. (**B**) The expression of brassinolide pathway enrichment genes in leaves and stalks. (**C**) The expression of gibberellin pathway enrichment genes in leaves and stalks.

4.3. Important Functional Genes Related to Density Tolerance

Stalk elongation has an important effect on the development of lateral organs such as leaves, and we found multiple DEGs affecting both stalk strength and leaf morphogenesis in the paper. The overexpression of *ATGA20OX1* increased maize leaf elongation and stalk internode length [48]. Similar results were found in this study, as the *ATGA20OX1* homologous genes Zm00001d034898, Zm00001d042611, and Zm00001d012212 were up-regulated in stalks and leaves (Supplementary Table S8), which may be responsible for the longer leaf length and internode length in NL409. Zm00001d013130 and Zm00001d033267 were involved in plant photomorphogenesis, and their knockdown attenuated the shade avoidance syndrome in maize [49]. Intriguingly, we found that the expression of Zm00001d013130 and Zm00001d033267 was down-regulated (Figure 9C). The Zm00001d039453 gene was highly expressed in the elongation phase of maize stalks, while the knockdown of this gene caused shorter internodes and a reduction in plant height [50], as well as affecting leaf morphology [51]. Consistent with these previous findings, Zm00001d039453 was significantly up-regulated in leaves and not significantly up-regulated in stalks (Supplementary Table S9). Meanwhile, Zm00001d039453 was shared

by GO and KEGG enrichment analyses (Supplementary Table S7) and co-expressed in the Turquoise module (Supplementary Table S14), further demonstrating the function of this gene. These genes discussed above may enhance the density tolerance of narrow-leaved maize inbred line NL409.

The identification of candidate genes for stalk strength can provide advice for marker-assisted breeding. Zm00001d037636 and Zm00001d037547 are candidate genes located in stem strength *pQTL6-1*, which are required for cellulose and lignin biosynthesis, and are involved in cell wall synthesis and digestion, respectively [52]. Intriguingly, the up-regulated expression of Zm00001d037636 and the down-regulated expression of Zm00001d037547 were identified in the stalks (Supplementary Table S12). This result indicates that these two genes may have contributed to the higher stalk strength of NL409 compared to WB665. Zm00001d005421 was also a candidate gene for stalk strength QTL [52], which up-regulated expression in the stiff-stalk line [34], and its overexpression could increase the leaf elongation rate [53]. Similar to the results of previous studies, we found that the expression of Zm00001d005421 was up-regulated in leaves and stalks (Supplementary Table S12). Moreover, Zm00001d037636 and Zm00001d005421 were co-expressed in the Turquoise and Red modules (Supplementary Tables S13 and S14) associated with leaf and stem development. These findings suggested that the genes mentioned above may be involved in the enhanced density tolerance of NL409, and these genes can be used in marker-assisted breeding for density tolerance.

In this study, eleven core genes were identified by WGCNA analysis, among which the transcription factor ZmCOL8 (Zm00001d013443, Figure 7) binding site was consistent with maize leaf width loci detected by GWAS analysis, and the knockdown of *ZmCOL8* resulted in a development-inhibited phenotype [54]. Our results were consistent with previous studies (Figure 1; Supplementary Tables S3 and S4). In addition, the expression of another core gene, Zm00001d000316 (Figure 7), was regulated by ZmbHLH43 and ZmGATA12 (Zm00001d037605) [55], while binding sites of the transcription factors ZmbHLH43 and ZmGATA12 were also consistent with the leaf width loci detected by GWAS analysis [54]. It has been reported that the expression of *ZmbHLH43* was regulated by *ZmHOX32*, which affected maize leaf morphology [56]. Meanwhile, *OsHOX32* affected cellulose and lignin biosynthesis [57], which may be related to stem strength. Our results showed that Zm00001d013443 and Zm00001d000316 were co-expressed in the Turquoise module (Supplementary Table S14). Therefore, we speculate that Zm00001d013443 and Zm00001d000316 play important roles in regulating leaf and stem development, but their molecular regulatory mechanisms need to be further clarified.

5. Conclusions

In this study, WGCNA analysis identified 11 hub genes highly related to leaf width and stalk strength. In addition, 28 stem-strength candidate genes and 13 cell wall digestion genes were detected. The differences in the expression of these genes related to cellulose, hemicellulose, lignin, and cell-wall formation might be the main factors contributing to the significant differences in leaf morphology and stalk strength between the two inbred maize lines. Intriguingly, we found that the expression of Zm00001d039453, Zm00001d037636, and Zm00001d005421 may be associated with enhanced density tolerance of the narrow leaf line. These findings can provide a theoretical basis for the narrow-leaf and high-strength stalk formation in high-density-tolerance maize and contribute to the proposal of a breeding strategy for yield improvement.

Supplementary Materials: The following supporting information can be downloaded at: https://www.mdpi.com/article/10.3390/agronomy14071506/s1, Figure S1: Auxin response elements in the promoter region of BR-responsive and biosynthetic genes; Figure S2: Heat map of cellulose, hemicellulose, and lignin candidate genes in leaves and stalks between the narrow-leaved maize inbred line NL409 and the wide-leaved maize inbred line WB665; Figure S3: Heat map of genes associated with cell wall loosening and hydrolysis in leaves and stalks between the narrow-leaved maize inbred line NL409 and the wide-leaved maize inbred line WB665; Table S1: Primer sequences

used for qRT-PCR analysis; Table S2: Quality of transcriptome sequencing data; Table S3: LDEGs identified in leaves between the narrow-leaved maize inbred line NL409 and the wide-leaved maize inbred line WB665; Table S4: SDEGs identified in stems between the narrow-leaved maize inbred line NL409 and the wide-leaved maize inbred line WB665; Table S5: GO enrichment analysis of DEGs identified in leaves and stalks between the narrow-leaved maize inbred line NL409 and the wide-leaved maize inbred line WB665; Table S6: KEGG analysis of DEGs identified in leaves and stalks between the narrow-leaved maize inbred line NL409 and the wide-leaved maize inbred line WB665; Table S7: Genes co-enriched by KEGG and GO analysis; Table S8: Plant hormone pathway related genes; Table S9: Plant hormone signal transduction and BR biosynthesis related genes; Table S10: Cellulose, hemicellulose, and lignin candidate genes; Table S11: Cell wall loosening and hydrolysis-related genes; Table S12: Stalk strength candidate genes; Table S13: Red co-expression module gene expression pattern; Table S14: Turquoise co-expression module gene expression pattern.

Author Contributions: S.G., X.Z. and X.L. conceived and designed the experiments. Y.G., Y.S., J.G. and Q.Z. performed the experiments, L.W. and Z.W. gave some good suggestions on the manuscript. S.G., J.Z., Y.G. and L.C. performed the data analysis and interpretation. S.G., J.Z. and Z.H. prepared the figures and tables. S.G. wrote the manuscript and provided the funding. All authors have read and agreed to the published version of the manuscript.

Funding: This research was funded by the National Natural Science Foundation of China (32001565), the Fund for Distinguished Young Scholars from Henan Academy of Agricultural Sciences (2023JQ06), the Excellent Youth Fund of Henan Academy of Agricultural Sciences (2020YQ14), and the Independent Innovation Project of Henan Academy of Agricultural Sciences (2023ZC128).

Data Availability Statement: The original contributions presented in the study are included in the article/Supplementary Materials, further inquiries can be directed to the corresponding author.

Conflicts of Interest: The authors declare no conflicts of interest.

References

1. Liu, G.Z.; Yang, H.S.; Xie, R.Z.; Yang, Y.S.; Liu, W.M.; Guo, X.X.; Xue, J.; Ming, B.; Wang, K.R.; Hou, P.; et al. Genetic gains in maize yield and related traits for high-yielding cultivars released during 1980s to 2010s in China. *Field Crops Res.* **2021**, *270*, 108223. [CrossRef]
2. Xue, J.; Xie, R.Z.; Zhang, W.F.; Wang, K.R.; Hou, P.; Ming, B.; Gou, L.; Li, S.K. Research progress on reduced lodging of high-yield and-density maize. *J. Integr. Agric.* **2017**, *16*, 2717–2725. [CrossRef]
3. Gou, L.; Huang, J.J.; Zhang, B.; Li, T.; Sun, R.; Zhao, M. Effects of population density on stalk lodging resistant mechanism and agronomic characteristics of Maize. *Acta Agron. Sin.* **2007**, *33*, 1688–1695. (In Chinese)
4. Xue, J.; Gou, L.; Shi, Z.G.; Zhao, Y.S.; Zhang, W.F. Effect of leaf removal on photosynthetically active radiation distribution in maize canopy and stalk strength. *J. Integr. Agric.* **2017**, *16*, 85–96. [CrossRef]
5. Baird, A.S.; Taylor, S.H.; Pasquet-Kok, J.; Vuong, C.; Zhang, Y.; Watcharamongkol, T.; Scoffoni, C.; Edwards, E.J.; Christin, P.A.; Osborne, C.P.; et al. Developmental and biophysical determinants of grass leaf size worldwide. *Nature* **2021**, *592*, 242–247. [CrossRef] [PubMed]
6. Pan, L.; George-Jaeggli, B.; Borrell, A.; Jordan, D.; Koller, F.; Al-Salman, Y.; Ghannoum, O.; Cano, F.J. Coordination of stomata and vein patterns with leaf width underpins water-use efficiency in a C4 crop. *Plant Cell Environ.* **2021**, *45*, 1612–1630. [CrossRef] [PubMed]
7. Evans, J.R.; Kaldenhoff, R.; Genty, B.; Terashima, I. Resistances along the CO_2 diffusion pathway inside leaves. *J. Exp. Bot.* **2009**, *60*, 2235–2248. [CrossRef] [PubMed]
8. Zhi, X.Y.; Hammer, G.; Borrell, A.; Tao, Y.F.; Wu, A.; Hunt, C.; Mace, E.; George-Jaeggli, B. Genetic basis of sorghum leaf width and its potential as a surrogate for transpiration efficiency. *Theor. Appl. Genet.* **2022**, *135*, 3057–3071. [CrossRef] [PubMed]
9. Qi, J.; Qian, Q.; Bu, Q.Y.; Li, S.Y.; Chen, Q.; Sun, J.Q.; Liang, W.X.; Zhou, Y.H.; Chou, C.C.; Li, X.G.; et al. Mutation of the rice Narrow leaf1 gene, which encodes a novel protein, affects vein patterning and polar auxin transport. *Plant Physiol.* **2008**, *147*, 1947–1959. [CrossRef] [PubMed]
10. Li, M.; Xiong, G.; Li, R.; Cui, J.; Tang, D.; Zhang, B.; Zhou, Y. Rice cellulose synthase-like D4 is essential for normal cell-wall biosynthesis and plant growth. *Plant J.* **2009**, *60*, 1055–1069. [CrossRef] [PubMed]
11. Li, W.; Yang, Z.X.; Yao, J.Y.; Li, J.S.; Song, W.B.; Yang, X.H. Cellulose synthase-like D1 controls organ size in maize. *BMC Plant Biol.* **2018**, *18*, 239. [CrossRef]
12. Jiang, F.; Guo, M.; Yang, F.; Duncan, K.; Jackson, D.; Rafalski, A.; Wang, S.C.; Li, B.L. Mutations in an AP2 Transcription Factor-Like Gene Affect Internode Length and Leaf Shape in Maize. *PLoS ONE* **2012**, *7*, e37040. [CrossRef] [PubMed]

13. Phillips, K.A.; Skirpan, A.L.; Liu, X.; Christensen, A.; Slewinsk, T.L.; Hudson, C.; Barazesh, S.; Cohen, J.D.; Malcomber, S.; McSteen, P. vanishing tassel2 encodes a grass-specific tryptophan aminotransferase required for vegetative and reproductive development in maize. *Plant Cell* **2011**, *23*, 550–566. [CrossRef] [PubMed]
14. Multani, D.S.; Briggs, S.P.; Chamberlin, M.A.; Murphy, A.S.; Jogal, A.G.S. Loss of an MDR transporter in compact stalks of maize br2 and sorghum dw3 mutants. *Science* **2003**, *302*, 81–84. [CrossRef] [PubMed]
15. Carraro, N.; Forestan, C.; Canova, S.; Traas, J.; Varotto, S. *ZmPIN1a* and *ZmPIN1b* encode two novel putative candidates for polar auxin transport and plant architecture determination of maize. *Plant Physiol.* **2006**, *142*, 254–264. [CrossRef] [PubMed]
16. Li, Z.X.; Zhang, X.R.; Zhao, Y.J.; Li, Y.J.; Zhang, G.F.; Peng, Z.H.; Zhang, J.R. Enhancing auxin accumulation in maize root tips improves root growth and dwarfs plant height. *Plant Biotechnol. J.* **2018**, *16*, 86–99. [CrossRef]
17. He, L.; Zhang, S.; Qiu, Z.N.; Zhao, J.; Nie, W.D.; Lin, H.Y.; Zhu, Z.G.; Zeng, D.L.; Qian, Q.; Zhu, L. FRUCTOKINASE-LIKE PROTEIN 1 interacts with TRXz to regulate chloroplast development in rice. *J. Integr. Plant Biol.* **2018**, *60*, 94–111. [CrossRef]
18. Lv, Y.S.; Shao, G.N.; Qiu, J.H.; Jiao, G.A.; Sheng, Z.H.; Xie, L.H.; Wu, Y.W.; Tang, S.Q.; Wei, X.J.; Hu, P.S. White Leaf and Panicle 2, encoding a PEP-associated protein, is required for chloroplast biogenesis under heat stress in rice. *J. Exp. Bot.* **2017**, *68*, 5147–5160. [CrossRef] [PubMed]
19. Bae, K.D.; Um, T.Y.; Yang, W.T.; Parkc, T.H.; Hong, S.Y.; Kim, K.M. Characterization of dwarf and narrow leaf (dnl-4) mutant in rice. *Plant Signal. Behav.* **2021**, *16*, 1849490. [CrossRef] [PubMed]
20. Han, L.L.; Jiang, C.G.; Zhang, W.; Wang, H.W.; Li, K.; Liu, X.G.; Liu, Z.F.; Wu, Y.J.; Huang, C.L.; Hu, X.J. Morphological Characterization and Transcriptome Analysis of New Dwarf and Narrow-Leaf (dnl2) Mutant in Maize. *Int. J. Mol. Sci.* **2022**, *23*, 795. [CrossRef]
21. Wang, X.; Zhang, R.Y.; Shi, Z.; Zhang, Y.; Sun, X.; Ji, Y.L.; Zhao, Y.X.; Wang, J.D.; Zhang, Y.X.; Xing, J.F.; et al. Multi-omics analysis of the development and fracture resistance for maize internode. *Sci. Rep.* **2019**, *9*, 8183. [CrossRef] [PubMed]
22. Romsdahl, T.B.; Cocuron, J.C.; Pearson, M.J.; Alonso, A.P.; Chapman, K.D. A lipidomics platform to analyze the fatty acid compositions of non-polar and polar lipid molecular species from plant tissues: Examples from developing seeds and seedlings of pennycress (*Thlaspi arvense*). *Front. Plant Sci.* **2022**, *13*, 1038161. [CrossRef] [PubMed]
23. Zheng, S.; Su, M.; Shi, Z.F.; Gao, H.X.; Ma, C.; Zhu, S.; Zhang, L.; Wu, G.F.; Wang, J.; Zhang, J.P.; et al. Exogenous sucrose influences KEA1 and KEA2 to regulate abscisic acid-mediated primary root growth in Arabidopsis. *Plant Sci.* **2022**, *317*, 111209. [CrossRef] [PubMed]
24. Brown, J.; Pirrung, M.; McCue, L.A. FQC Dashboard: Integrates FastQC results into a web-based, interactive, and extensible FASTQ quality control tool. *Bioinformatics* **2017**, *33*, 3137–3139. [CrossRef] [PubMed]
25. Jiao, Y.; Peluso, P.; Shi, J.; Liang, T.; Stitzer, M.C.; Wang, B.; Campbell, M.S.; Stein, J.C.; Wei, X.; Chin, C.-S.; et al. Improved maize reference genome with single-molecule technologies. *Nature* **2017**, *546*, 524–527. [CrossRef] [PubMed]
26. Kim, D.; Langmead, B.; Salzberg, S. HISAT: A fast spliced aligner with low memory requirements. *Nat. Methods* **2015**, *12*, 357–360. [CrossRef] [PubMed]
27. Trapnell, C.; Williams, B.A.; Pertea, G.; Mortazavi, A.; Kwan, G.; Baren, M.J.; Woid, B.J.; Pachter, L. Transcript assembly and quantification by RNA-Seq reveals unannotated transcripts and isoform switching during cell differentiation. *Nat. Biotechnol.* **2010**, *28*, 511–515. [CrossRef] [PubMed]
28. Love, M.; Huber, W.; Anders, S. Moderated estimation of fold change and dispersion for RNA-seq data with DESeq2. *Genome Biol.* **2014**, *15*, 550. [CrossRef] [PubMed]
29. Yu, G.; Wang, L.; Han, Y.; He, Q. clusterProfiler: An R package for comparing biological themes among gene clusters. *Omics-J. Integr. Biol.* **2012**, *16*, 284–287. [CrossRef]
30. Langfelder, P.; Horvath, S. WGCNA: An R package for weighted correlation network analysis. *BMC Plant Biol.* **2008**, *9*, 559. [CrossRef] [PubMed]
31. Wang, X.T.; Wu, L.J.; Zhang, S.F.; Wu, L.C.; Ku, L.X.; Wei, X.M.; Chen, Y.H. Robust expression and association of *ZmCCA1* with circadian rhythms in maize. *Plant Cell Rep.* **2011**, *30*, 1261–1272. [CrossRef] [PubMed]
32. Livak, K.J.; Schmittgen, T.D. Analysis of relative gene expression data using real-time quantitative PCR and the $2^{-\Delta\Delta CT}$ method. *Methods* **2001**, *25*, 402–408. [CrossRef]
33. Zhao, Y.T.; Zhang, S.; Lv, Y.J.; Ning, F.F.; Cao, Y.B.; Liao, S.H.; Wang, P.; Huang, S.B. Optimizing ear-plant height ratio to improve kernel number and lodging resistance in maize (*Zea mays* L.). *Field Crops Res.* **2022**, *276*, 108376. [CrossRef]
34. Zhang, Z.H.; Zhang, X.; Lin, Z.L.; Wang, J.; Liu, H.Q.; Zhou, L.N.; Zhong, S.Y.; Li, Y.; Zhu, C.; Lai, J.S.; et al. A large transposon insertion in the stiff1 promoter increases stalk strength in maize. *Plant Cell.* **2020**, *32*, 152–165. [CrossRef]
35. Manga-Robles, A.; Santiago, R.; Malvar, R.A.; Moreno-González, V.; Fornalé, S.; López, I.; Encina, A.; García-Angulo, P. Elucidating compositional factors of maize cell walls contributing to stalk strength and lodging resistance. *Plant Sci.* **2021**, *307*, 110882. [CrossRef] [PubMed]
36. Zhang, X.H.; Liu, H.; Zhou, G.Y.; Ruan, H.Q.; Cui, H.W.; Pang, J.L.; Khan, U.S.; Zong, N.; Wang, R.Z.; Leng, P.F.; et al. Genome-wide association study and metabolic pathway prediction of barrenness in maize as a response to high planting density. *J. Integr. Agric.* **2022**, *21*, 3514–3523. [CrossRef]
37. Dohmann, E.M.N.; Nill, C.; Schwechheimer, C. DELLA proteins restrain germination and elongation growth in Arabidopsis thaliana COP9 signalosome mutants. *Eur. J. Cell Biol.* **2010**, *89*, 163–168. [CrossRef] [PubMed]

38. Li, P.H.; Ponnala, L.; Gandotra, N.; Wang, L.; Si, Y.Q.; Tausta, S.L.; Kebrom, T.H.; Provart, N.; Patel, R.; Myers, C.R.; et al. The developmental dynamics of the maize leaf transcriptome. *Nat. Genet.* **2010**, *42*, 1060–1067. [CrossRef]
39. Wang, S.L.; Zhang, F.; Jiang, P.F.; Zhang, H.; Zhang, H.; Cheng, R.H.; Xu, Z.T.; Ikram, A.U.; Li, E.Z.; Xu, Z.S.; et al. SDG128 is involved in maize leaf inclination. *Plant J.* **2021**, *108*, 1597–1608. [CrossRef] [PubMed]
40. Ren, Z.B.; Liu, Y.R.; Li, L.; Wang, X.; Zhou, Y.Y.; Zhang, M.C.; Li, Z.H.; Yi, F.; Duan, L.S. Deciphering transcriptional mechanisms of maize internodal elongation by regulatory network analysis. *J. Exp. Bot.* **2023**, *74*, 4503–4519. [CrossRef] [PubMed]
41. Nicolas, M.; Cubas, P. The Role of TCP Transcription Factors in Shaping Flower Structure, Leaf Morphology, and Plant Architecture. In *Plant Transcription Factors*; Academic Press: Cambridge, MA, USA, 2016; pp. 249–267.
42. Guo, Z.X.; Fujioka, S.; Blancaflor, E.B.; Miao, S.; Gou, X.P.; Li, J. TCP1 modulates brassinosteroid biosynthesis by regulating the expression of the key biosynthetic gene DWARF4 in Arabidopsis thaliana. *Plant Cell* **2010**, *22*, 1161–1173. [CrossRef] [PubMed]
43. Nicolas, M.; Cubas, P. TCP factors: New kids on the signaling block. *Curr. Opin. Plant Biol.* **2016**, *33*, 33–41. [CrossRef]
44. Schruff, M.C.; Spielman, M.; Tiwari, S.; Adams, S.; Fenby, N.; Scott, R.J. The AUXIN RESPONSE FACTOR 2 gene of Arabidopsis links auxin signalling, cell division, and the size of seeds and other organs. *Development* **2006**, *133*, 251–261. [CrossRef] [PubMed]
45. Cancé, C.; Martin-Arevalillo, R.; Boubekeur, K.; Dumas, R. Auxin response factors are keys to the many auxin doors. *New Phytol.* **2022**, *235*, 402–419. [CrossRef]
46. Jiao, S.P.; Hazebroek, J.P.; Chamberlin, M.A.; Perkins, M.; Sandhu, A.S.; Gupta, R.; Simcox, K.D.; Li, Y.H.; Prall, A.; Heetland, L.; et al. Chitinase-like Plays a Role in Stalk Tensile Strength in Maize. *Plant Physiol.* **2019**, *181*, 1127–1147. [CrossRef] [PubMed]
47. Xie, Y.L.; Wen, D.; Wu, C.L.; Zhang, C.Q. Transcriptome analysis reveals the mechanism of internode development affecting maize stalk strength. *BMC Plant Biol.* **2022**, *22*, 49. [CrossRef]
48. Nelissen, H.; Rymen, B.; Jikumaru, Y.; Demuynck, K.; Lijsebettens, M.V.; Kamiya, Y.; Inzé, D.; Beemster, G.T.S. A local maximum in gibberellin levels regulates maize leaf growth by spatial control of cell division. *Curr. Biol.* **2012**, *22*, 1183–1187. [CrossRef] [PubMed]
49. Shi, Q.B.; Kong, F.; Zhang, H.S.; Jiang, Y.; Heng, S.Q.; Liang, R.; Liu, J.H.; Lu, X.D.; Li, P.H.; Li, G. Molecular mechanisms governing shade responses in maize. *Biochem. Biophys. Res. Commun.* **2019**, *516*, 112–119. [CrossRef]
50. Le, L.; Guo, W.; Du, D.; Zhang, X.; Wang, W.; Yu, J.; Pu, L. A spatiotemporal transcriptomic network dynamically modulates stalk development in maize. *Plant Biotechnol. J.* **2022**, *20*, 2313–2331. [CrossRef]
51. Ren, Z.Z.; Wu, L.C.; Ku, L.X.; Wang, H.T.; Zeng, H.; Su, H.H.; Zhang, D.L.; Han, S.B.; Chen, Y.H. ZmILI1 regulates leaf angle by directly affecting liguleless1 expression in maize. *Plant Biotechnol. J.* **2020**, *18*, 881–883. [CrossRef]
52. Liu, X.G.; Hu, X.J.; Li, K.; Liu, Z.F.; Wu, Y.J.; Wang, H.W.; Huang, C.L. Genetic mapping and genomic selection for maize stalk strength. *BMC Plant Biol.* **2020**, *20*, 196. [CrossRef] [PubMed]
53. Ding, L.; Milhiet, T.; Couvreur, V.; Nelissen, H.; Meziane, A.; Parent, B.; Aesaert, S.; Lijsebettens, M.V.; Inzé, D.; Tardieu, F.; et al. Modification of the expression of the aquaporin ZmPIP2; 5 affects water relations and plant growth. *Plant Physiol.* **2020**, *182*, 2154–2165. [CrossRef] [PubMed]
54. Tu, X.; Mejía-Guerra, M.; Valdes Franco, J.; Tzeng, D.; Chu, P.; Shen, W.; Li, P.H.; Buckler, E.S.; Zhong, S.L. Reconstructing the maize leaf regulatory network using ChIP-seq data of 104 transcription factors. *Nat. Commun.* **2020**, *11*, 5089. [CrossRef] [PubMed]
55. Chang, Y.M.; Lin, H.H.; Liu, W.Y.; Li, W.H. Comparative transcriptomics method to infer gene coexpression networks and its applications to maize and rice leaf transcriptomes. *Proc. Natl. Acad. Sci. USA* **2019**, *116*, 3091–3099. [CrossRef]
56. Miao, X.X.; Zhu, W.C.; Jin, Q.X.; Song, Z.Z.; Li, L. ZmHOX32 is related to photosynthesis and likely functions in plant architecture of maize. *Front. Plant Sci.* **2023**, *14*, 1119678. [CrossRef]
57. Chen, H.; Fang, R.Q.; Deng, R.F.; Li, J.X. The OsmiRNA166b-OsHox32 pair regulates mechanical strength of rice plants by modulating cell wall biosynthesis. *Plant Biotechnol. J.* **2021**, *19*, 1468–1480. [CrossRef] [PubMed]

Disclaimer/Publisher's Note: The statements, opinions and data contained in all publications are solely those of the individual author(s) and contributor(s) and not of MDPI and/or the editor(s). MDPI and/or the editor(s) disclaim responsibility for any injury to people or property resulting from any ideas, methods, instructions or products referred to in the content.